Arch Toxicol
DOI 10.1007/s00204-016-1793-9

INORGANIC COMPOUNDS

Epidermal growth factor prevents thallium(I)- and thallium(III)-mediated rat pheochromocytoma (PC12) cell apoptosis

María Teresa Luján Pino[1] · Clarisa Marotte[1] · Sandra Viviana Verstraeten[1]

Received: 27 January 2016 / Accepted: 5 July 2016

Abstract We have reported recently that the proliferation of PC12 cells exposed to micromolar concentrations of Tl(I) or Tl(III) has different outcomes, depending on the absence (EGF^- cells) or the presence (EGF^+ cells) of epidermal growth factor (EGF) added to the media. In the current work, we investigated whether EGF supplementation could also modulate the extent of Tl(I)- or Tl(III)-induced cell apoptosis. Tl(I) and Tl(III) (25–100 μM) decreased cell viability in EGF^- but not in EGF^+ cells. In EGF^- cells, Tl(I) decreased mitochondrial potential, enhanced H_2O_2 generation, and activated mitochondrial-dependent apoptosis. In addition, Tl(III) increased nitric oxide production and caused a misbalance between the anti- and pro-apoptotic members of Bcl-2 family. Tl(I) increased ERK1/2, JNK, p38, and p53 phosphorylation in EGF^- cells. In these cells, Tl(III) did not affect ERK1/2 and JNK phosphorylation but increased p53 phosphorylation that was related to the promotion of cell senescence. In addition, this cation significantly activated p38 in both EGF^- and EGF^+ cells. The specific inhibition of ERK1/2, JNK, p38, or p53 abolished Tl(I)-mediated EGF^- cell apoptosis. Only when p38 activity was inhibited, Tl(III)-mediated apoptosis was prevented in EGF^- and EGF^+ cells. Together, current results indicate that EGF partially prevents the noxious effects of Tl by preventing the sustained activation of MAPKs signaling cascade that lead cells to apoptosis and point to p38 as a key mediator of Tl(III)-induced PC12 cell apoptosis.

Keywords Thallium · Epidermal growth factor · Cell signaling · Apoptosis · MAPK · p38

Abbreviations

Ac-DEVD-pNA	*N*-acetyl-Asp-Glu-Val-Asp *p*-nitroanilide
Ac-IETD-pNA	*N*-acetyl-Ile-Glu-Thr-Asp *p*-nitroanilide
ASK-1	Apoptosis signal-regulating kinase 1
Bax	Bcl-2-associated X protein
Bcl-2	B-cell lymphoma 2
DHR123	Dihydrorhodamine 123
DMEM	Dulbeccós modified Eagle medium
2,4-DNP	2,4-dinitrophenol
EGF	Epidermal growth factor
ERK	Extracellular signal-regulated kinases
IOD	Integrated optical density
JNK	c-Jun N-terminal kinase
L-NAME	$L\text{-}N^G$-nitroarginine methyl ester
MAPK	Mitogen-activated protein kinase
MAPKKK	MAPK kinase kinase
MTT	3-(4,5-Dimethylthiazol-2-yl)-2,5-diphenyl-tetrazolium bromide
NEDA	*N*-(1-naphtyl)ethylenediamine dihydrochloride
NO	Nitric oxide
NOS	Nitric oxide synthase
PARP	Poly(AD ribose) polymerase
PI	Propidium iodide
PBS	Phosphate-buffered saline
PR	Ponceau red
R123	Rhodamine 123

Electronic supplementary material The online version of this article (doi:10.1007/s00204-016-1793-9) contains supplementary material, which is available to authorized users.

✉ Sandra Viviana Verstraeten
verstraeten@ffyb.uba.ar

[1] Consejo Nacional de Investigaciones Científicas y Técnicas (CONICET), Instituto de Química y Fisicoquímica Biológicas (IQUIFIB), Facultad de Farmacia y Bioquímica, Universidad de Buenos Aires, Buenos Aires, Argentina

Published online: 13 July 2016

ROS	Reactive oxygen species
SA-β-Gal	Senescence-associated-β-galactosidase
TBS	Tris-buffered saline
X-Gal	5-Bromo-4-chloro-3-indolyl β-D-galactoside

Introduction

The heavy metal thallium (Tl) is a normal component of the Earth's crust, although its bioavailability is limited due to the formation of scarcely soluble salts and minerals. However, upon its mobilization through mining and its disposal as industrial waste, the air, water, and soils became contaminated with this metal (for a review, see ATSDR 1999; Cheam 2001; Law and Turner 2011). Moreover, certain regions of the world are naturally enriched in Tl (Cvjetko et al. 2010). In consequence, edible plant cultivars grown in Tl-rich soils accumulate Tl in their roots and leaves (Wierzbicka et al. 2004; Xiao et al. 2004; Pavlickova et al. 2006; Queirolo et al. 2009), and the metal becomes available to humans (Bunzl et al. 2001; Heim et al. 2002). In addition to this route, human exposure to Tl occurs via dermal contact with Tl-containing compounds or the inhalation of airborne particles (Repetto et al. 1998; Peter and Viraraghavan 2005).

Tl can be found in either of two oxidation states, the monovalent (Tl(I)) or the trivalent (Tl(III)) cations. The high oxidant potential of Tl(III) (Tl(III)/Tl(I) ε°: +1.25 V) confers this cation strong oxidant capacity. Thus, upon its interaction with biological molecules, Tl(III) can oxidize them and alter their structure and/or functionality. It has been demonstrated in rats that ^{201}Tl(I) and ^{201}Tl(III) distribute equally among the different organs, being the kidneys, testis, and brain the organs with the highest contents of Tl (Sabbioni et al. 1981). This pattern of distribution is in accordance with the clinical manifestations of chronic Tl exposure that includes renal failure and alterations in the peripheral and central nervous systems (Schaub 1996; Galvan-Arzate and Santamaria 1998; Heim et al. 2002; Cvjetko et al. 2010). Despite knowing the clinical symptoms caused by Tl(I) accumulation, the molecular mechanisms underlying its toxicity, along with those of Tl(III), remain to be elucidated.

Aimed to clarify the molecular events involved in Tl(I) and Tl(III) toxicity, we performed a series of studies using rat pheochromocytoma (PC12) cells as model. These cells were chosen since they share similarities with sympathetic neurons, as they synthesize, store, and release catecholamines (Chen et al. 1994). The neural crest embryological origin of PC12 cells (Fujita et al. 1989) makes them a good model for the study of the events involved in the proliferation and differentiation of neuronal precursors (Greene and Tischler 1976; Fujita et al. 1989), as well as for the assessment of potentially neurotoxic agents. Using PC12 cells, we demonstrated that Tl(I) and Tl(III) (10–100 μM) alter their redox state (Hanzel and Verstraeten 2006), activate the mitochondrial and/or the extrinsic pathways of apoptosis (Hanzel and Verstraeten 2009), and destabilize lysosomes (Hanzel et al. 2012). In addition, we reported recently that Tl(I) and Tl(III) have differential effects on the progression of PC12 cell cycle (Pino and Verstraeten 2015), which were modulated by the presence of the epidermal growth factor (EGF) in the media. PC12 cell stimulation with EGF activates transiently the Ras → Raf → MEK1/2 → ERK1/2 signaling cascade, which induces cell proliferation (Henson and Gibson 2006). Prior to their use, cell growth was stopped by serum deprivation, and cell cycle reentry was stimulated by serum replenishment either in the absence (EGF^- cells) or in the presence (EGF^+ cells) of EGF (10 ng/ml) and Tl(I) or Tl(III) (10–100 μM). We found that these cations did not activate per se the EGF receptor in EGF^- cells, but induced ERK1/2 and Akt activation, both pathways being involved in the initial steps of cell proliferation. Supporting that Tl(I) promoted the proliferation in both EGF^- and EGF^+ cells. In contrast, while Tl(III) promoted EGF^- cell proliferation, it delayed the progress of the cycle in EGF^+ cells (Pino and Verstraeten 2015). In the present work, we continued the latter study investigating the hypothesis that, in addition to act as a mitogen, EGF might also prevent the activation of the cellular events that prime cells to apoptosis upon Tl exposure. Obtained results indicate that EGF prevents almost completely the pro-apoptotic effects of Tl(I) and Tl(III) by preventing the sustained activation of the mitogen-activated protein kinases (MAPKs) ERK1/2, JNK, and p38, as well as p53 activation in Tl-exposed cells.

Materials and methods

Chemicals

Dulbeccós modified Eagle medium (DMEM high glucose), horse serum, and Hank's balanced salt solution were purchased from Gibco BRL (Grand Island, NY, USA). Fetal bovine serum was from Natocor (Córdoba, Argentina). Thallium(I) nitrate was from Fluka (Milwaukee, WI, USA). Thallium(III) trinitrate was from Alfa Æsar (Ward Hill, MA, USA). Murine epidermal growth factor (EGF) was from PeproTech Inc. (Rocky Hill, NJ, USA). The fluorescent probes rhodamine 123 (R123) and dihydrorhodamine 123 (DHR123) were obtained from Invitrogen–Molecular Probes (Eugene, OR, USA). The following primary antibodies and the appropriate horseradish peroxidase-conjugated secondary antibodies were from

Santa Cruz Biotechnology (Santa Cruz, CA, USA): Bax (sc-526), Bcl-XL (sc-8392), Fas (sc-1023), JNK1/2 (sc-572), p38 (sc-535), p53 (sc-55476), poly(ADP ribose) polymerase (PARP, sc-7150), β-tubulin (sc-55529) and actin (sc-1616). Monoclonal primary antibodies against Bcl-2 (#2876), phospho-Bcl-2 (Ser_{70}, #2871), ERK1/2 (#9102), phospho-ERK1/2 (Thr_{202}/Tyr_{204}, #4370), phospho-JNK1/2 (Tyr_{183}/Tyr_{185}, #4668), phospho-p38 (Thr_{180}/Tyr_{182}, #4511) and phospho-p53 (Ser_{15}, #9284) were from Cell Signaling Technology Inc. (Danvers, MA, USA). Caspase 3 (Ac-DEVD-pNA) and caspase 8 (Ac-IETD-pNA) substrates, and the inhibitors of JNK (SP600125), ERK1/2 (PD98059), p38 (SB203580) and p53 (pifithrin-α) were obtained from Enzo Life Sciences, Inc. (Farmingdale, NY, USA). CHAPS and the enhanced chemiluminescence system (Pierce® ECL plus) for Western immunoblot was from Thermo Scientific (Rockford, IL, USA). Complete, EDTA-free protease inhibitor and PhosStop phosphatase inhibitor cocktails were from Roche Diagnostics GmbH (Mannheim, Germany). Etoposide (Euvaxon®) was from Tuteur SACIFIA (Buenos Aires, Argentina). PVDF membranes were from Bio-Rad Corp. (Hercules, CA, USA). Ribonuclease A from bovine pancreas (RNAse), propidium iodide (PI), 2,4-dinitrophenol (DNP), Hoechst 32258, Neutral red, 5-bromo-4-chloro-3-indolyl β-D-galactoside (X-Gal), *N*-(1-naphtyl)ethylenediamine dihydrochloride (NEDA), sulfanilic acid, and all the other reagents had the highest quality available and were from Sigma-Aldrich (St. Louis, MO, USA).

Tl solutions

Tl(I) and Tl(III) stock solutions were prepared as described previously (Hanzel and Verstraeten 2006). The amounts of Tl(I) or Tl(III) used in the experiments did not affect the pH of the culture medium.

Cell culture and incubations

PC12 cells were obtained from the American Type Culture Collection (ATCC, Rockville, MD, USA) and cultured in complete medium (DMEM supplemented with 10 % horse serum, 5 % fetal bovine serum, 100 units/ml of penicillin G, 100 μg/ml of streptomycin, and 4 mM L-glutamine) at 37 °C in a 5 % CO_2 atmosphere (Hanzel and Verstraeten 2006). All experiments were performed using cell cultures between passages 10 and 25.

Cells were harvested by 5-min incubation at 37 °C in the presence of sterile 0.125 % (w/v) trypsin, 0.02 % (w/v) disodium EDTA in Hank's balanced salt solution (pH 7.2). As indicated for the individual experiments, cells were seeded on sterile, poly-L-lysine-treated 6-, 48- or 96-well plates (3×10^6, 5×10^5, and 6×10^4 cells per well, respectively), or 60- or 100-mm culture dishes (3×10^6 and 1×10^7 cells per dish, respectively), and allowed to grow until ~60 % of confluence. Cell growth was stopped by serum deprivation for 24 h. Next, the culture medium was replaced by complete medium without (EGF^- cells) or with (EGF^+ cells) the addition of 10 ng/ml EGF, and with or without the simultaneous addition of Tl(I) or Tl(III) (10–100 μM) (Pino and Verstraeten 2015). Cells were harvested and processed as indicated for the individual experiments.

Mitochondrial functionality

Mitochondrial functionality was evaluated from MTT reduction (Mosmann 1983). PC12 cells were grown on 96-well plates and incubated in the conditions described above. At the end of incubation, samples were added with MTT solution (0.05 mg/ml in sterile phosphate-buffered saline, PBS) and incubated for 1 h at 37 °C. Formazan crystals were solubilized in 10 % (w/v) SDS in HCl 0.01 N, and the absorbance at 570 nm (reference 630 nm) was measured in a Rayto RT-2100C microplate reader (Rayto Life and Analytical Sciences Co., Shenzhen, P.R. China). Results were expressed as the percentage of the values measured in control cells. As positive control, EGF^- and EGF^+ cells were incubated for 24 h in the presence of 50 μg/ml sodium etoposide.

Lysosomal integrity

Lysosomal integrity was evaluated from Neutral red uptake (Repetto et al. 2008). PC12 cells were grown on 96-well plates and incubated in the conditions described above. Samples were added with 8 μg/ml Neutral red in PBS and further incubated for 2 h at 37 °C. After incubation, cells were washed twice with warm PBS. Intracellular Neutral red was solubilized in 0.150 ml of freshly prepared destain solution (48 % absolute ethanol, 51 % distilled water, 1 % glacial acetic acid), and the absorbance was measured at 540 nm in a microplate reader. Raw data were normalized by protein content in the samples as described by Ciapetti et al. (1996). Briefly, cells were washed three times with warm PBS to eliminate the Neutral red dye and fixed for 15 min at room temperature with 0.1 ml of 1 % (v/v) glutaraldehyde in PBS. Samples were incubated for 30 min at room temperature with 0.1 ml of 0.1 % (w/v) amido black in 0.1 M sodium acetate, 1.515 M acetic acid buffer (pH 3.5). Unbound amido black was removed by washing cells twice with acid distilled water (pH 3.5–5), and protein-bound amido black was eluted with 0.150 ml of 50 mM NaOH. The absorbance of the samples was measured at 630 nm (reference 405 nm) in a microplate reader. Neutral red uptake was calculated as the ratio between Neutral red and amido black absorbance. As positive control,

EGF^- and EGF^+ cells were incubated for 24 h in the presence of 50 μg/ml sodium etoposide.

Plasma membrane integrity

Cell plasma membrane integrity was evaluated from the binding of propidium iodide (PI) to DNA in the absence of detergents (Verstraeten 2006). PC12 cells were grown on 96-well plates apt for fluorescence measurements and incubated in the conditions described above. Samples were added with 25 μM propidium iodide (PI) and incubated for 5 min at room temperature and in the dark. The fluorescence corresponding to PI-DNA complex was measured at 590 nm (λexcitation: 538 nm) in a PerkinElmer LS-55 spectrofluorometer (PerkinElmer Ltd., Beaconsfield, UK). Cells were next disrupted incubating the samples for 30 min at 37 °C in the presence of 0.1 % (v/v) Igepal in PBS, and maximal PI-DNA complex formation was measured. Results were expressed as the ratio between PI-DNA fluorescence measured in the absence and in the presence of the detergent. As positive control, EGF^- and EGF^+ cells were incubated for 24 h in the presence of 50 μg/ml sodium etoposide.

Evaluation of mitochondrial membrane potential

Mitochondrial membrane potential was evaluated measuring the incorporation of the fluorescent probe R123 (Rago et al. 1992). PC12 cells were grown on 96-well plates apt for fluorescence measurements and incubated in the conditions described above. Samples were added with 10 μM R123 and incubated at 37 °C for 20 min. Cells were washed twice with pre-warmed PBS and disrupted for 30 min at 37 °C with Igepal (0.1 % v/v) in PBS. R123 fluorescence was measured at 530 nm (λexcitation: 507 nm). Samples were next added with 25 μM PI and further incubated for 10 min in the dark, and DNA content was estimated as described above. Results were expressed as the ratio between R123 and PI fluorescence. As positive control, EGF^- and EGF^+ cells were incubated for 30 min in the presence of 100 μM 2,4-dinitrophenol (DNP).

Evaluation of mitochondrial oxidant content

The steady-state content of mitochondrial oxidants was evaluated as described previously (Hanzel and Verstraeten 2006). PC12 cells were grown on 96-well plates apt for fluorescence measurements and incubated in the conditions described above. Samples were added with 5 μM DHR123 and incubated at 37 °C for 30 min. Cells were washed twice with PBS, disrupted with Igepal (0.1 % v/v) in PBS, and fluorescence emission was measured at 535 nm (λexcitation: 525 nm). Samples were next added with 5 μM of the intercalating agent Hoechst 32258 and further incubated for 10 min in the dark. DNA content was estimated from the fluorescence intensity of DNA-Hoechst complex at 420 nm (λexcitation: 370 nm). Results were expressed as the ratio between DHR123 and Hoechst 32258 fluorescence. As positive control, EGF^- and EGF^+ cells were incubated for 30 min in the presence of 100 μM 2,4-dinitrophenol (DNP).

Evaluation of extracellular nitrite content

PC12 cells were grown on 48-well plates and incubated for 24 h in the conditions described above. Culture media were separated and centrifuged at $800\times g$ for 5 min, and nitrite content was evaluated in the supernatants (Guevara et al. 1998). Aliquots containing 0.1 ml of samples were transferred to 96-well plates and incubated for 5 min at room temperature in the presence of sulfanilic acid (0.33 %, w/v) in 5 % (v/v) H_3PO_4. Samples were next added with 0.025 % (w/v) NEDA and further incubated for 15 min at room temperature in the dark. The absorbance of samples was recorded at 550 nm in a microplate reader. The concentration of nitrite in the samples was calculated from a standard curve run in parallel, using freshly prepared sodium nitrite. Results were normalized by the amount of cells in the samples, using a standard curve of known amounts of PC12 cells determined by the trypan blue exclusion method and measured with the fluorescent probe Hoechst 32258 as described.

Determination of caspase 3 and 8 activities

Caspase 3 and 8 activities were evaluated in whole-cell lysates (Hanzel and Verstraeten 2009). Cells were grown on 6-well plates, incubated in the conditions described above, and exposed to 100 μM Tl(I) or Tl(III) for 24 h. Cells were collected by scrapping in warm PBS and centrifuged for 10 min at $1000\times g$ at 4 °C. Pellets were suspended in a 50 mM HEPES buffer (pH 7.4) containing 0.1 % (w/v) CHAPS, 1 mM DTT, 0.1 mM EDTA, and 150 mM NaCl, 1 mM PMSF, and protease and phosphatase inhibitor cocktails, and incubated on ice for 30 min. Samples were centrifuged at $12000 \times g$ for 10 min at 4 °C. Protein content was measured in supernatants (Bradford 1976), and samples were stored at −80 °C until their use. Aliquots containing 5 μl of the samples were incubated for 3 h at 37 °C in the presence of 0.2 ml of the same buffer added with 10 % (v/v) glycerol and 40 μM of the corresponding substrate (caspase 3: Ac-DEVD-pNA; caspase 8: Ac-IETD-pNA). The formation of *p*-nitroanilide was recorded every 30 min at 405 nm in a microplate reader. Caspases activities were expressed as pmol of *p*-nitroanilide min^{-1} μg $protein^{-1}$.

Determination of hypodiploid cell content

The relative amount of cells with hypodiploid DNA content was determined as described by Nicoletti et al. (1991). PC12 cells were grown on 60-mm-diameter dishes and incubated for 30 h in the conditions described above. Cells were collected by scrapping, centrifuged at 800×*g* for 10 min at 4 °C, and washed twice with pre-warmed PBS. Cells were suspended in 1 ml of fixing solution containing 70 % (v/v) ethanol and 0.5 % (v/v) Tween-20 in PBS, and kept at 4 °C for at least 24 h. Samples were centrifuged at 800×*g* for 10 min at 4 °C, washed twice with PBS, suspended in 0.1 ml of a solution containing 50 μM PI and 0.1 mg/ml DNAse-free RNAse, and further incubated at room temperature for 30 min. Cell aggregates were disrupted by filtering samples through a 0.2-μM-pore nylon mesh. DNA content in the samples was evaluated in a FacsCalibur flow cytometer (Becton–Dickinson, Mountain View, CA, USA), equipped with a 488-nm laser and recorded in FL2 channel (585 nm). Acquired raw data were analyzed using the software WinMDI 2.9 (http://www.cyto.purdue.edu/flowcyt/software/Winmdi.htm).

Preparation of cell fractions for Western blot analysis

PC12 cells were grown on 100-mm-diameter culture dishes and incubated for 24 h in the conditions described above. Cells were washed twice with pre-warmed PBS, collected by scrapping, centrifuged at 800×*g* for 10 min at 4 °C, and pellets were frozen for at least 1 h at −80 °C. Whole-cell lysates were obtained as described previously (Hanzel and Verstraeten 2009). Samples were added with protease and phosphatase inhibitor cocktails to prevent protein degradation during their manipulation and storage. After protein quantification (Bradford 1976), samples were stored at −80 °C until their use.

Western blot analysis

Proteins were separated by reducing SDS-PAGE electrophoresis and transferred to PVDF membranes. Colored molecular weight standards (GE Healthcare, Piscataway, NJ, USA) were ran simultaneously. Membranes were blocked for 1 h in 5 % (w/v) bovine serum albumin in Tris-buffered saline containing 0.1 % (v/v) Tween-20 and incubated overnight at 4 °C in the presence of the corresponding primary antibody. The following dilutions of antibodies were used: ERK1/2 1:2,000; p-ERK1/2, JNK1/2, p38, Fas, β-tubulin and actin 1:1000; p-p53 1:750; SOD2, Bcl-2, Bcl-XL, Bax, PARP, p-JNK1/2, p-p38 and p53 1:500; p-Bcl-2: 1:200. Membranes were further incubated for 90 min with the corresponding peroxidase-conjugated secondary antibody (dilution 1:10,000). Specific bands were revealed with chemiluminescent Pierce® ECL plus Western blot substrate (Thermo Scientific, IL, USA) and detected using Amersham Hyperfilm ECL (GE Healthcare Bio-Sciences, PA, USA). Raw data were analyzed using Gel-Pro Analyzer 4.0 (Media Cybernetics Inc., Bethesda, MD, USA).

Evaluation of cell senescence

Cell senescence was evaluated as described by Dimri et al. (1995) from the activity of senescence-associated β-galactosidase (SA-β-Gal). PC12 cells were grown on 48-well plates and incubated for 24 h in the conditions described above. After incubation, culture media were discarded, samples were washed twice with warm PBS, and cells were fixed at room temperature for 5 min with 2 % (w/v) formaldehyde and 0.2 % (w/v) glutaraldehyde. Samples were washed twice with PBS and incubated for 24 h at 37 °C in the presence of a staining solution containing 1 mg/ml X-Gal, 5 mM potassium ferrocyanide, 5 mM potassium ferricyanide, 2 mM $MgCl_2$ and 150 mM NaCl in 40 mM citric acid, 120 mM Na_2HPO_4 buffer (pH 6.0). Samples were washed twice with PBS and observed through a Nikon Eclipse TE300 inverted microscope (Nikon Instruments Inc., Tokyo, Japan) coupled with an Accu-Scope 519CU Micrometrics CMOS Digital Camera (Accu-Scope Inc., NY, USA) at 400X magnification. Senescent cells were identified from the presence of blue precipitate in cell cytoplasm corresponding to metabolized X-Gal. Results were expressed as the percentage of X-Gal positive cells respect to total cells in the field. At least 1000 cells were counted for each experimental condition.

Statistics

The effects of EGF on PC12 cells were analyzed by Student's *t* test. The effects of Tl(I) and Tl(III) were analyzed by one-way analysis of variance (ANOVA) followed by Fisher's protected least square difference test. The comparison between the effects of Tl(I) and Tl(III) was performed by two-way ANOVA followed by Bonferroni's posttest. All statistical analyses were performed using the routines available in GraphPad Prism version 6.00 for Windows, GraphPad Software (San Diego, CA, USA). A probability (*P*) value <0.05 was considered statistically significant.

Results

Effect of EGF on Tl(I)- and Tl(III)-mediated alterations in cell viability

PC12 cells were synchronized in G_0/G_1 phase by serum deprivation for 24 h, and cell cycle reentry was achieved

by serum replenishment either with (EGF^+ cells) or without (EGF^- cells) the addition of 10 ng/ml EGF (Pino and Verstraeten 2015). Since Tl(I) and Tl(III) decreased cell viability in non-synchronized PC12 cells (Hanzel and Verstraeten 2006), the possibility that these cations may also alter cell viability in the current experimental model was first investigated. To fulfill this objective, three different parameters were evaluated: mitochondrial functionality, plasma membrane integrity, and lysosomal functionality.

After 24 h of cell cycle reentry, basal MTT metabolization in EGF^- and EGF^+ cells achieved similar values (MTT absorbance: 0.584 ± 0.015 and 0.574 ± 0.017, respectively), indicating similar mitochondrial functionality in both cell populations. In EGF^- cells, Tl(I) and Tl(III) decreased MTT metabolization in a concentration-dependent manner (Fig. 1a, b). In the 25–50 μM range of concentrations, the magnitudes of the effects due to Tl(I) and Tl(III) were similar. However, at 100 μM concentration, the effect due to Tl(III) (−45 %, $P < 0.001$ respect to controls) was significantly higher than that of Tl(I) ($P < 0.001$). Tl(I) affected MTT reduction in EGF^- and EGF^+ cells to a similar extent (Fig. 1a). In contrast, the effect of 100 μM Tl(III) on MTT reduction was only partially prevented by EGF ($P < 0.001$) (Fig. 1b). For comparative purposes, EGF^- and EGF^+ cells were also exposed for 24 h to the pro-apoptotic compound etoposide (50 μg/ml) but in the absence of Tl. MTT metabolization was significantly decreased ($P < 0.001$) in these cells (EGF^- cells: −43 %, EGF^+ cells: −22 %) (Suppl. Figure 1A), the magnitude of the effect caused by etoposide being similar to that caused by Tl(III) in EGF^- cells.

To assess whether the lower capacity to metabolize MTT of Tl-exposed cells was associated with the impairment of other cell vital functions, lysosomes ability to incorporate and retain the dye Neutral red was investigated. Tl(I) decreased Neutral red uptake in EGF^- cells in a concentration-dependent manner, the effect being significant only at the highest concentration assessed (−20 %, $P < 0.01$; Fig. 1c). Similarly, Tl(III) decreased Neutral

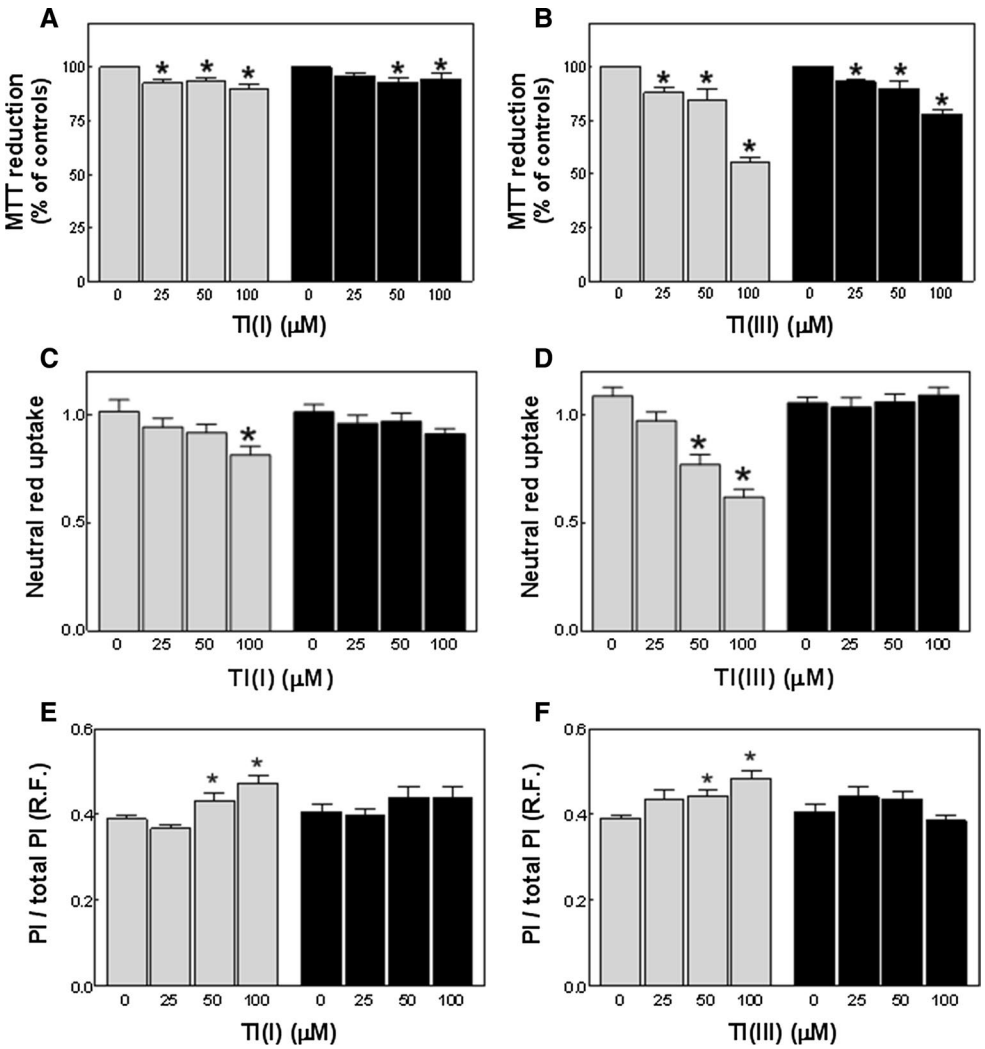

Fig. 1 EGF prevents Tl-induced loss of cell viability. PC12 cells were incubated at 37 °C for 24 h in serum-free DMEM. After media replacement, EGF^- (*white bar*) and EGF^+ (*black bar*) cells were further incubated for 24 h in the presence of 25–100 μM **a**, **c**, **e** Tl(I) or **b**, **d**, **f** Tl(III). Cell viability was evaluated from **a**, **b** mitochondrial capacity to metabolize MTT, **c**, **d** lysosome capacity to incorporate Neutral red, and **e**, **f** plasma membrane capacity to exclude PI. Results are shown as the mean ± SEM of at least four independent experiments. *Asterisk* significantly different from the value measured in control cells ($P < 0.001$). *RF* relative fluorescence

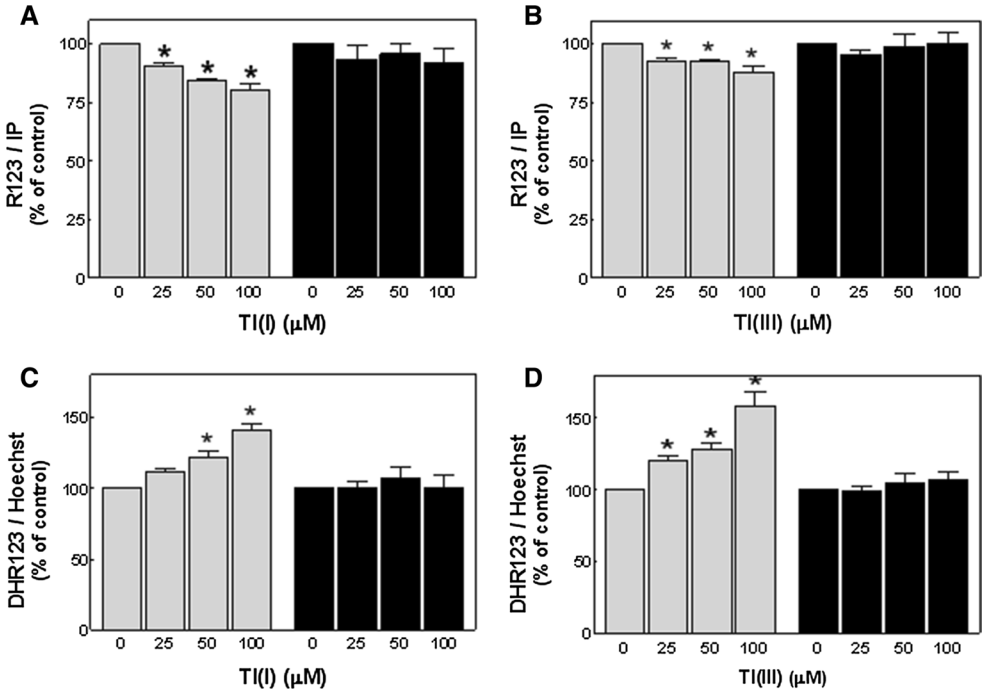

Fig. 2 EGF prevents Tl-induced mitochondrial depolarization and oxidants production. PC12 cells were incubated at 37 °C for 24 h in serum-free DMEM. After media replacement, EGF^- (*white bar*) and EGF^+ (*black bar*) cells were incubated for 24 h in the presence of 25–100 μM **a**, **c** Tl(I) or **b**, **d** Tl(III), and **a**, **b** mitochondrial potential and **c**, **d** oxidant content were evaluated. Results are shown as the percentage of the value measured in cells incubated in the absence of Tl and are the mean ± SEM of five independent experiments. *Asterisk* denotes a significant difference from the value measured in control cells ($P < 0.001$)

red uptake only in EGF^- cells (−29 to −43 %; $P < 0.001$) (Fig. 1d). In these cells, the magnitude of the effect achieved at 100 μM Tl(III) was significantly higher than the observed in 100 μM Tl(I)-exposed cells ($P < 0.05$). EGF supplementation prevented Tl-mediated loss of Neutral red uptake (Fig. 1c, d). Etoposide caused 37 and 47 % decrease in Neutral red uptake in EGF^- and EGF^+ cells, respectively ($P < 0.001$; Suppl. Figure 1B), the magnitude of the effect being similar to the attained in EGF^- cells exposed to 100 μM Tl(III). To evaluate whether Tl also affected the integrity of the plasma membrane, the exclusion of the vital dye PI was measured. In EGF^- cells, Tl(I) and Tl(III) (50–100 μM) significantly increased ($P < 0.01$) the amount of cells with altered plasma membrane integrity, as evidenced from the increase in PI binding in the absence of the detergent Igepal (Fig. 1e, f). This effect was not observed in EGF^+ cells exposed to Tl(I) or Tl(III). Under the current experimental conditions, etoposide affected plasma membrane integrity both in EGF^- and EGF^+ cells (Suppl. Figure 1C), the magnitude of its effect being significantly higher than the observed in Tl-exposed cells ($P < 0.001$).

Together, these results suggest that, upon the exposure to Tl(I) or Tl(III), the viability of EGF^- cells is compromised, as evidenced by the decreased mitochondrial and lysosomal functionalities, accompanied by a partial loss of the integrity of the plasma membrane. The presence of EGF in culture media prevented Tl-mediated decrease in cell viability, supporting a protective role of this growth factor on Tl-dependent cytotoxicity.

Effect of EGF on Tl(I)- and Tl(III)-mediated promotion of apoptosis

It has been demonstrated that Tl(I) and Tl(III) induced mitochondrial depolarization in non-synchronized PC12 cells, with the consequent increase in the steady-state contents of H_2O_2 (Hanzel and Verstraeten 2006). On this basis, we next investigated the possibility that the impairment of mitochondrial capacity to metabolize MTT found in Tl-treated EGF^- cells could be associated with alterations in mitochondrial membrane potential and/or with the promotion of oxidant generation, and if those effects could be prevented by EGF.

Basal mitochondrial potentials of EGF^- and EGF^+ cells were similar, as evidenced from the uptake of the fluorescent probe R123 (Suppl. Figure 2A). To assess the sensitivity of the method, 24 h after cell cycle reentry, a subset of EGF^- and EGF^+ cells was incubated for 30 min in the presence of the mitochondrial uncoupler DNP (100 μM). As expected, DNP significantly decreased ($P < 0.01$) the uptake of R123 in EGF^- and EGF^+ cells (Suppl. Figure 2A), indicative of mitochondrial membrane depolarization. In EGF^- cells, Tl(I) and Tl(III) (25–100 μM) also decreased the uptake of R123 ($P < 0.01$ respect to controls; Fig. 2a, b). The magnitude of the effect caused by Tl(I) was markedly higher than that of Tl(III) ($P < 0.01$). In contrast, none of the cations affected R123 uptake in EGF^+ cells, suggesting that mitochondrial potential was preserved. Next, the steady-state concentration of mitochondrial oxidants was evaluated from the oxidation of

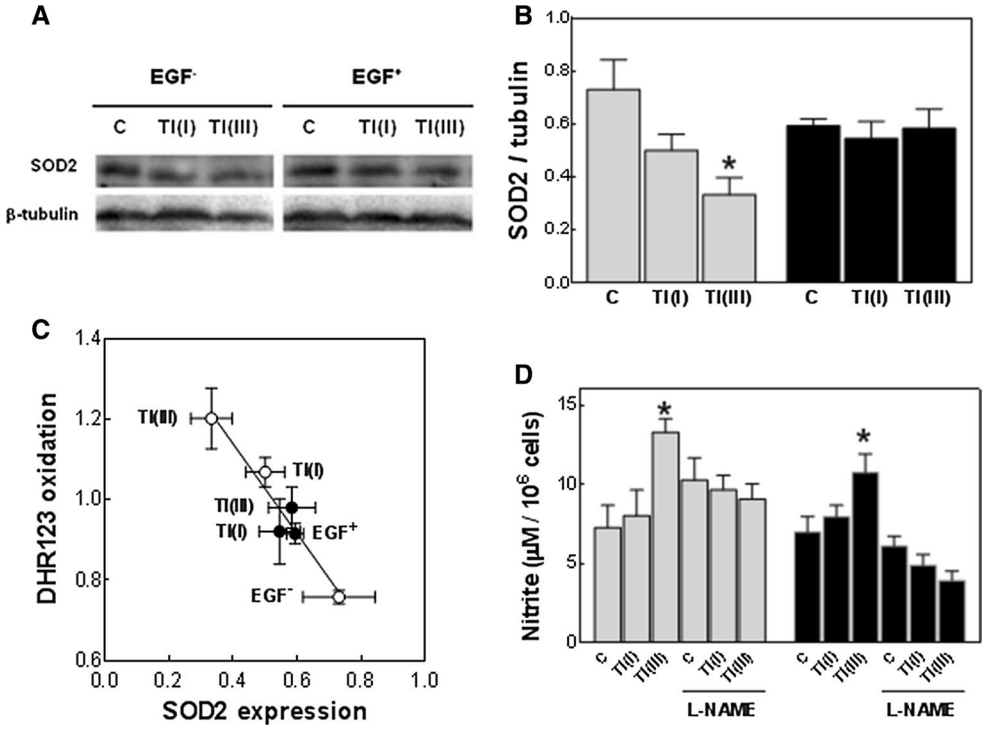

Fig. 3 EGF prevents Tl(III)-induced decrease in SOD2 expression and nitrite release. PC12 cells were incubated at 37 °C for 24 h in serum-free DMEM. After media replacement, EGF^- and EGF^+ cells were incubated for further 24 h in the presence of 100 μM Tl(I) or Tl(III), and SOD2 expression and nitrite release to the culture media were evaluated. **a** Representative Western blots showing the regions of the membrane corresponding to SOD2 (25 kDa) and β-tubulin (55 kDa) migration. **b** SOD2 expression relative to β-tubulin content in EGF^- (*white bar*) and EGF^+ (*black bar*) cells. **c** Correlation between DHR123 oxidation and SOD2 expression in EGF^- (*open circle*) and EGF^+ (*filled circle*) cells exposed to 100 μM Tl(I) or Tl(III). **d** Nitrite content in the culture media of EGF^- (*white bar*) and EGF^+ (*black bar*) cells exposed to Tl(I) or Tl(III) and either without or with the addition of 1 mM L-NAME. Results are shown the mean ± SEM of at least four independent experiments. *Asterisk* denotes a significant difference from the value measured in control cells ($P < 0.001$)

the probe DHR123. In EGF^+ cells, basal oxidation of DHR123 was 20 % higher than the value measured in EGF^- cells ($P < 0.001$; Suppl. Figure 2B). After 30 min of cell exposure to 100 μM DNP, DHR123 oxidation was significantly increased ($P < 0.001$) in EGF^- (+42 %) and EGF^+ (+27 %) cells (Suppl. Figure 2B). Tl(I) and Tl(III) increased DHR123 oxidation in EGF^- cells in a concentration-dependent manner (Fig. 2b, c), an effect that was not observed in EGF^+ cells.

To investigate the source of the oxidants evidenced by DHR123, we next evaluated the expression of SOD2, the enzyme that catalyzes the transformation of superoxide anion into H_2O_2 in the mitochondria. A tendency toward lower basal SOD2 expression was observed in EGF^+ cells respect to EGF^- cells (−19 %, $P = 0.05$) (Fig. 3a, b). In EGF^- cells exposed to 100 μM Tl(I) or Tl(III), the expression of SOD2 was 31 and 54 % lower than in controls ($P < 0.05$), respectively (Fig. 3b). In contrast, no significant changes in SOD2 expression were observed in EGF^+ cells exposed to Tl(I) or Tl(III). A significant and inverse relationship between SOD2 expression and DHR123 oxidation ($r^2 = 0.94$, $P < 0.005$) was observed (Fig. 3c). Tl(III) increased nitrite content in the culture media from EGF^- cells (83 %, $P < 0.001$) and EGF^+ cells (54 %, $P < 0.05$), an effect that was prevented by nitric oxide synthase inhibitor L-NAME (Fig. 3d). Tl(I) did not affect the concentration of nitrite in the culture media regardless the absence or presence of EGF (Fig. 3d).

We next investigated whether Tl(I) and/or Tl(III) could alter the expression of the main mitochondrial-related anti-apoptotic (Bcl-2 and Bcl-XL) and pro-apoptotic (Bax) members of the Bcl-2 family (Fig. 4a). In EGF^- cells, 100 μM Tl(I)—but not Tl(III)—significantly increased Bcl-2 expression (P < 0.01; Fig. 4b). However, the extent of Bcl-2 phosphorylation was similar for all the conditions assessed (Fig. 4c). The higher Bcl-2 expression in Tl(I)-treated EGF^- cells was compensated by decreased expression of Bcl-XL (−36 %; Fig. 4d). In contrast, Bax expression was increased in both Tl(I)- and Tl(III)-treated EGF^- cells, although the effect was significant only for the latter cation ($P < 0.01$). Therefore, the ratio between the anti-apoptotic and pro-apoptotic Bcl-2 family members

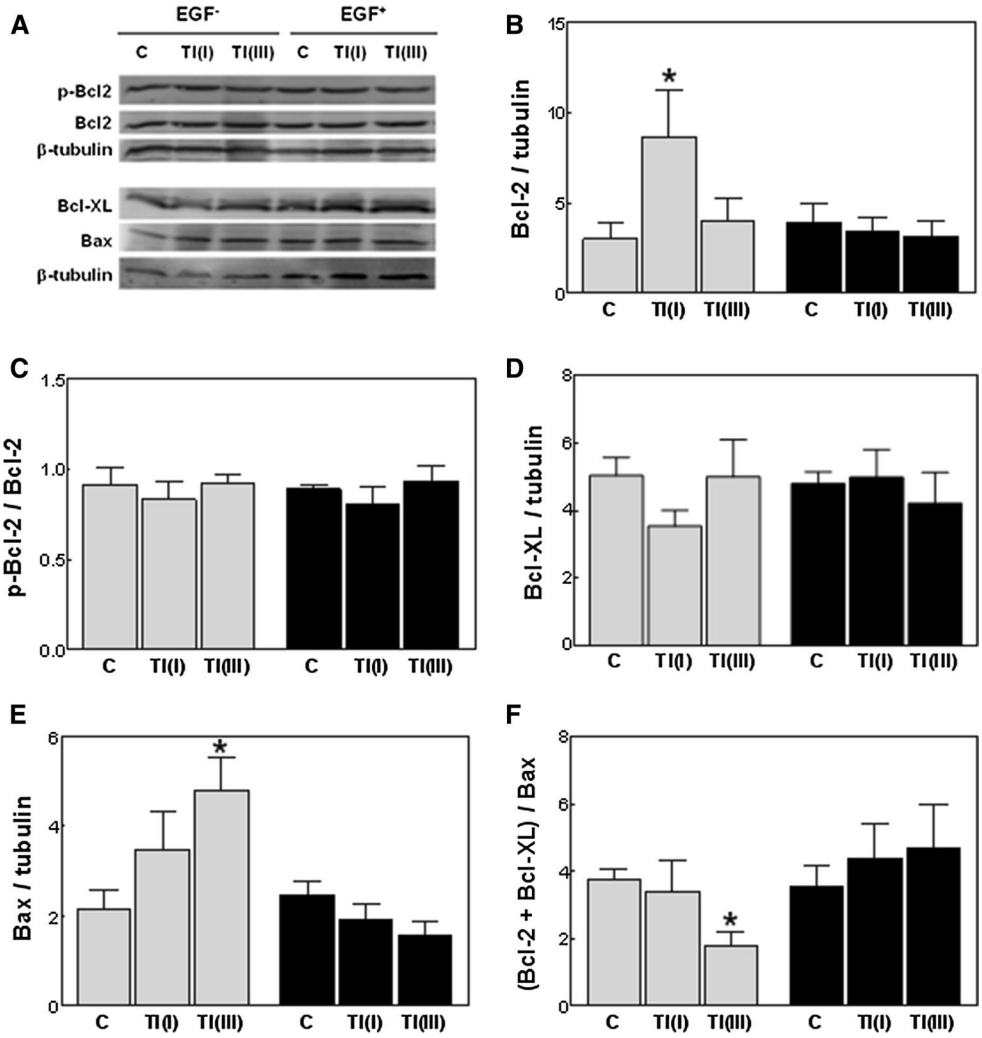

Fig. 4 EGF prevents Tl-induced misbalanced expression of Bcl-2 protein family. PC12 cells were incubated at 37 °C for 24 h in serum-free DMEM. After media replacement, EGF^- (*white bar*) and EGF^+ (*black bar*) cells were further incubated for 24 h in the presence of 100 μM Tl(I) or Tl(III). Phospho-Bcl-2 (p-Bcl-2), Bcl-2, Bcl-XL and Bax expression levels were evaluated. **a** Representative Western blots showing the regions of the membranes corresponding to p-Bcl-2 and Bcl-2 (28 kDa), Bcl-XL (30 kDa), Bax (23 kDa) and β-tubulin (55 kDa) migration. **b** Bcl-2 expression relative to β-tubulin content. **c** Bcl-2 activation, calculated as the ratio between p-Bcl-2 and total Bcl-2 expression levels.**d**, **e** Bcl-XL and Bax expression relative to β-tubulin content. **f** Relative content of anti-apoptotic (Bcl-2 and Bcl-XL) and pro-apoptotic (Bax) members of Bcl-2 protein family. Results are expressed as the mean ± SEM of at least four independent experiments. *Asterisk* denotes a significant difference from the value measured in control cells ($P < 0.01$)

was markedly decreased in Tl(III)-treated EGF^- cells, and close to control values in Tl(I)-treated cells (Fig. 4f). In EGF^+ cells, neither Tl(I) nor Tl(III) affected Bcl-2, Bcl-XL, and Bax expression (Fig. 4b, d, e), and the balance between anti- and pro-apoptotic Bcl-2 family members was thus preserved (Fig. 4f).

In non-synchronized PC12 cells, Tl(III)—but not Tl(I)—induced Fas expression, an effect that was related to the induction of the extrinsic pathway of apoptosis (Hanzel and Verstraeten 2009). Likewise, Fas expression levels were significantly higher in 100 μM Tl(III)-treated EGF^- cells (+61 %, $P < 0.01$), while its expression in Tl(I)-treated cells remained within control values (Fig. 5a, b). EGF supplementation significantly reduced Fas expression in Tl(III)-exposed cells (−70 %, $P < 0.01$). In line with the increased Fas expression observed in Tl(III)-treated EGF^- cells, the activity of caspase-8 was also increased (+87 %, $P < 0.01$; Fig. 5c). Tl(I) affected caspase 8 activity in neither EGF^+ nor EGF^- cells. The activity of the executioner caspase-3 was increased in EGF^- cells exposed to 100 μM Tl(I) or Tl(III), but not in EGF^+ cells submitted to similar conditions (Fig. 5d). Supporting that PARP cleavage, which is mediated by caspase-3, was increased in EGF^- but not in EGF^+ cells exposed to Tl (Fig. 5e, f). Finally, the amount of hypodiploid ($subG_1$) cells was evaluated by flow cytometry in PI-stained nuclei. After 30 h of cell cycle reentry, the amounts of apoptotic nuclei were 7±1 and 12±1 % in EGF^- and EGF^+ cells, respectively ($P < 0.01$). At this time point, both Tl(I) and Tl(III) increased the amount of apoptotic nuclei in EGF^- cells ($P < 0.001$ respect to controls) in a concentration-dependent manner (Fig. 5g, h). In contrast, the relative amount of apoptotic cells in Tl(I) (25–100 μM)- or Tl(III) (25–50 μM)-treated EGF^+ cells remained within control values. At 100 μM Tl(III), the number of apoptotic nuclei in EGF^+ cells was significantly increased respect to controls (+100 %, $P < 0.005$), the magnitude of the effect being significantly lower than the measured in EGF^- cells incubated in similar conditions ($P < 0.01$). The effects of Tl(I) and Tl(III) on the promotion of apoptosis in EGF^- cells were similar to the attained

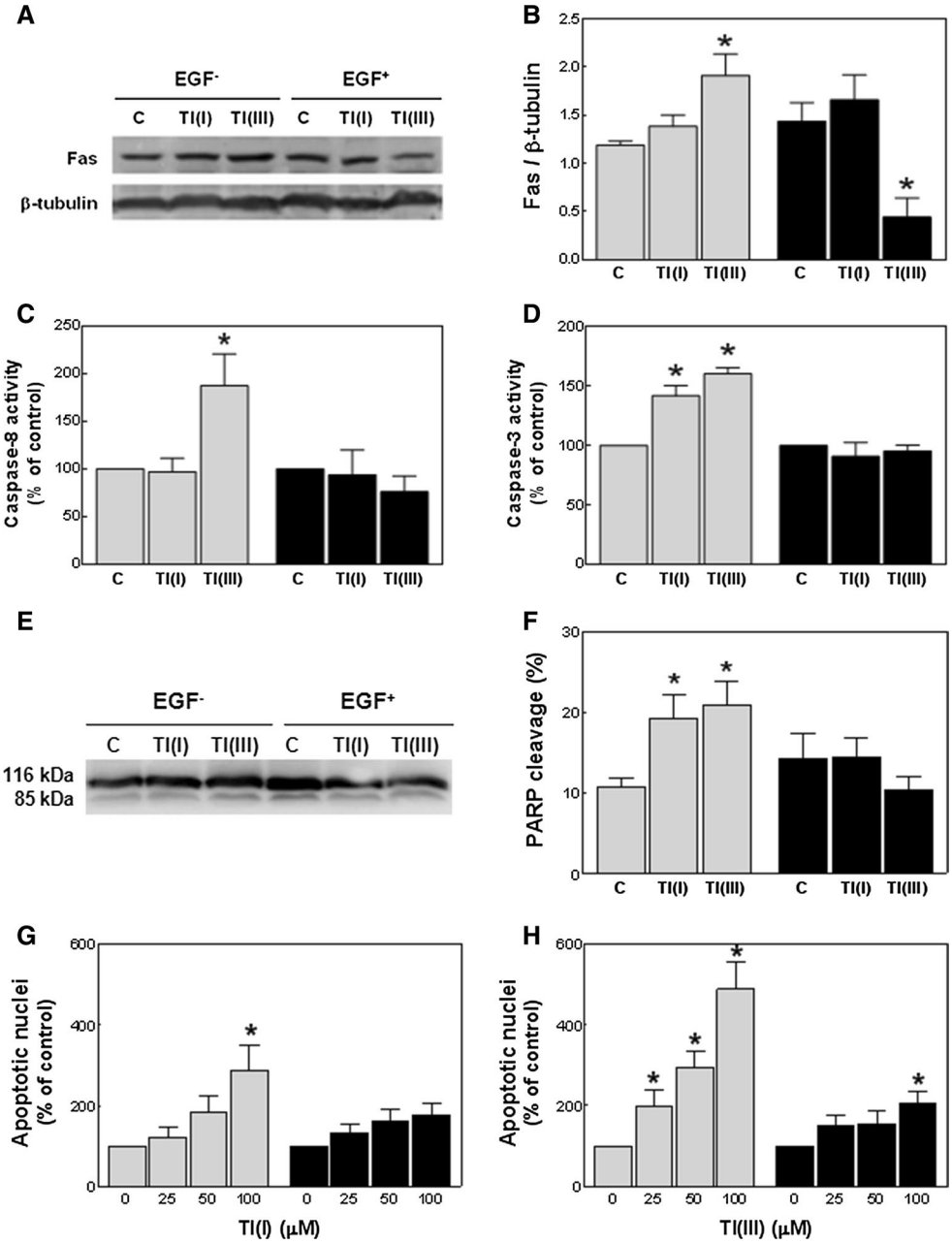

Fig. 5 EGF prevents Tl-induced cell apoptosis. PC12 cells were incubated at 37 °C for 24 h in serum-free DMEM. After media replacement, EGF^- (*white bar*) and EGF^+ (*black bar*) cells were further incubated for 24 h in the absence or presence of 100 μM Tl(I) or Tl(III). Fas expression in control and in Tl-treated cells. **a** Representative Western blot showing the regions of the membranes corresponding to Fas (48 kDa) and β-tubulin (55 kDa) migration. **b** Relative Fas expression respect to β-tubulin content. Caspase-8 **(c)** and caspase-3 **(d)** activities were measured in Tl(I)- and Tl(III)-treated cells, and results were expressed as the percentage of the value measured in control cells. PARP cleavage in control and in Tl-treated cells. **e** Representative Western blot showing the bands corresponding to full length (116 kDa) and cleaved (85 kDa) PARP. **f** PARP cleavage in the samples was calculated as $IOD_{85kDa}/(IOD_{85kDa} + IOD_{116kDa})$. Amount of hypodiploid cells evaluated by flow cytometry after 30 h of EGF^- and EGF^+ cell exposure to 25–100 μM **g** Tl(I) or **h** Tl(III) and expressed as the percentage of the value measured in control cells. Results are shown as the mean ± SEM of at least four independent experiments. *Asterisk* denotes a significant difference from the value measured in cells incubated in the absence of Tl ($P < 0.001$)

after cell exposure to 50 μg/ml etoposide (Suppl. Figure 3). In contrast to the observed for the effects of Tl, EGF was unable to prevent etoposide-mediated apoptosis (Suppl. Figure 3).

Participation of MAPKs and p53 in Tl-mediated apoptosis and senescence

To investigate whether Tl-mediated apoptosis was related to a sustained activation of the MAPKs, the phosphorylation of ERK1/2, JNK, and p38 was analyzed after 24 h of cell cycle reentry.

In the absence of Tl, p-ERK1/2 levels were similar in EGF^- and EGF^+ cells (Fig. 6a, b). In EGF^- cells, only 100 μM Tl(I) significantly increased p-ERK1/2 levels (+30 %, $P < 0.01$; Fig. 6b), with no significant variations observed in Tl(III)-exposed cells (Fig. 6c). In EGF^+ cells, ERK1/2 phosphorylation remained within control values for all the situations assessed (Fig. 6b, c). A tendency (+69 %, $P = 0.05$) toward higher basal levels of phosphorylated JNK was observed in EGF^+ cells (Fig. 6d). In EGF^- cells, Tl(I)—but not Tl(III)—significantly increased JNK phosphorylation (+150 to +190 %, $P < 0.01$; Fig. 6d, e). Neither Tl(I) nor Tl(III) affected JNK phosphorylation

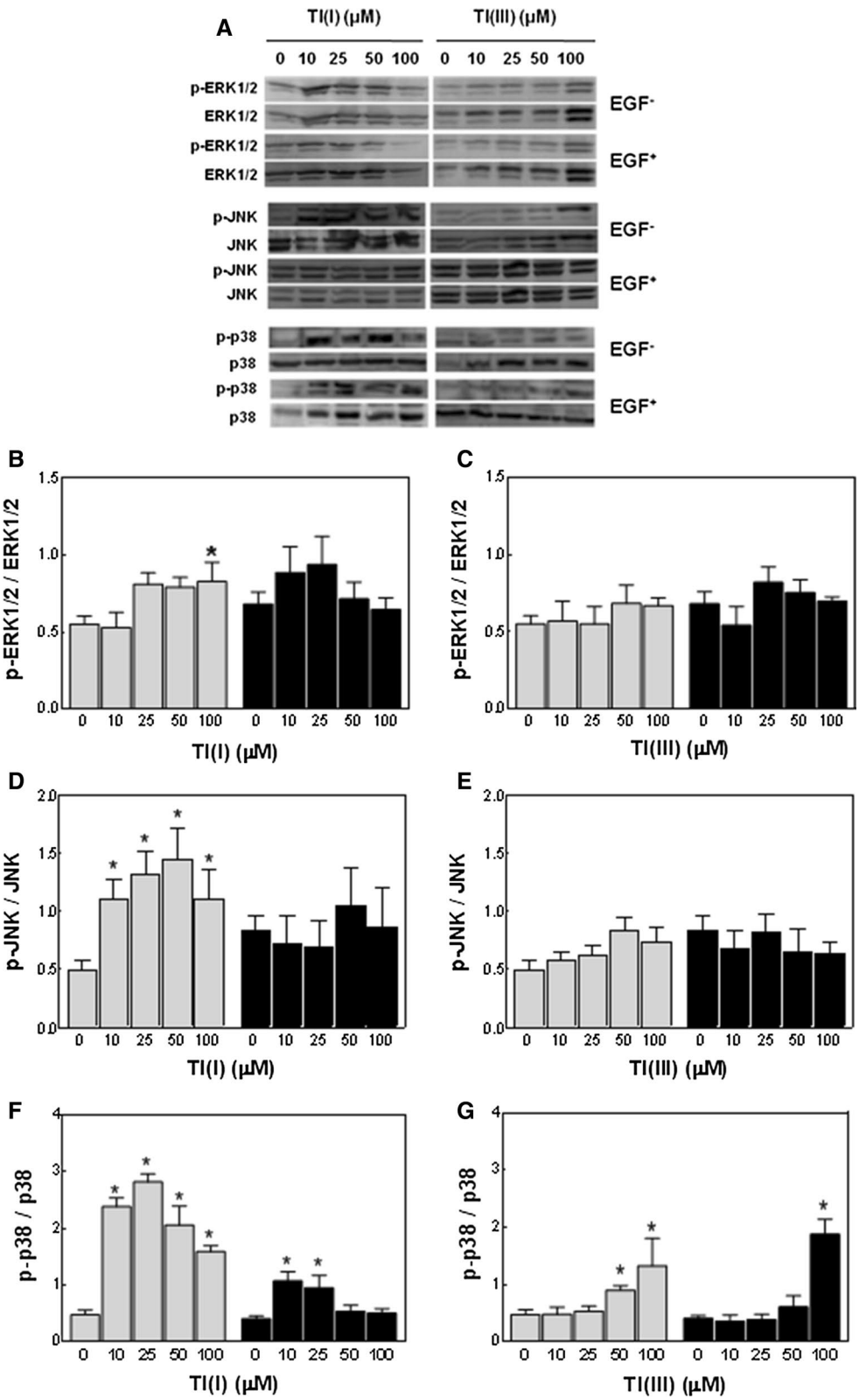

Fig. 6 EGF prevents Tl-induced phosphorylation of ERK1/2, JNK, and p38. PC12 cells were incubated at 37 °C for 24 h in serum-free DMEM. After media replacement, EGF^{-} (*white bar*) and EGF^{+} (*black bar*) cells were further incubated for 24 h in the presence of 10–100 μM Tl(I) or Tl(III), and the levels of phosphorylated ERK1/2 (p-ERK1/2), total ERK1/2, phosphorylated JNK (p-JNK), total JNK, phosphorylated p38 (p-p38), and total p38 were evaluated. **a** Representative Western blots showing the regions of the membrane corresponding to ERK (42 and 44 kDa), JNK (46 and 54 kDa), and p38 (40 and 43 kDa) migration. Relative p-ERK1/2 to total ERK1/2 expression content in **b** Tl(I)- or **c** Tl(III)-treated cells. Relative p-JNK to total JNK expression in **d** Tl(I)- or **e** Tl(III)-treated cells. Relative p-p38 to p38 expression levels in **f** Tl(I)- or **g** Tl(III)-treated cells. Results are shown as the mean ± SEM of at least four independent experiments. *Asterisk* denotes a significant difference from the value measured in control cells ($P < 0.001$)

in EGF^{+} cells along the range of concentrations assessed (Fig. 6d, e). Basal levels of phosphorylated p38 were similar in EGF^{-} and EGF^{+} cells (Fig. 6f, g). In EGF^{-} cells, both Tl(I) and Tl(III) significantly increased p38 phosphorylation ($P < 0.01$ respect to the controls), the magnitude of the effect due to Tl(I) being significantly higher than that of

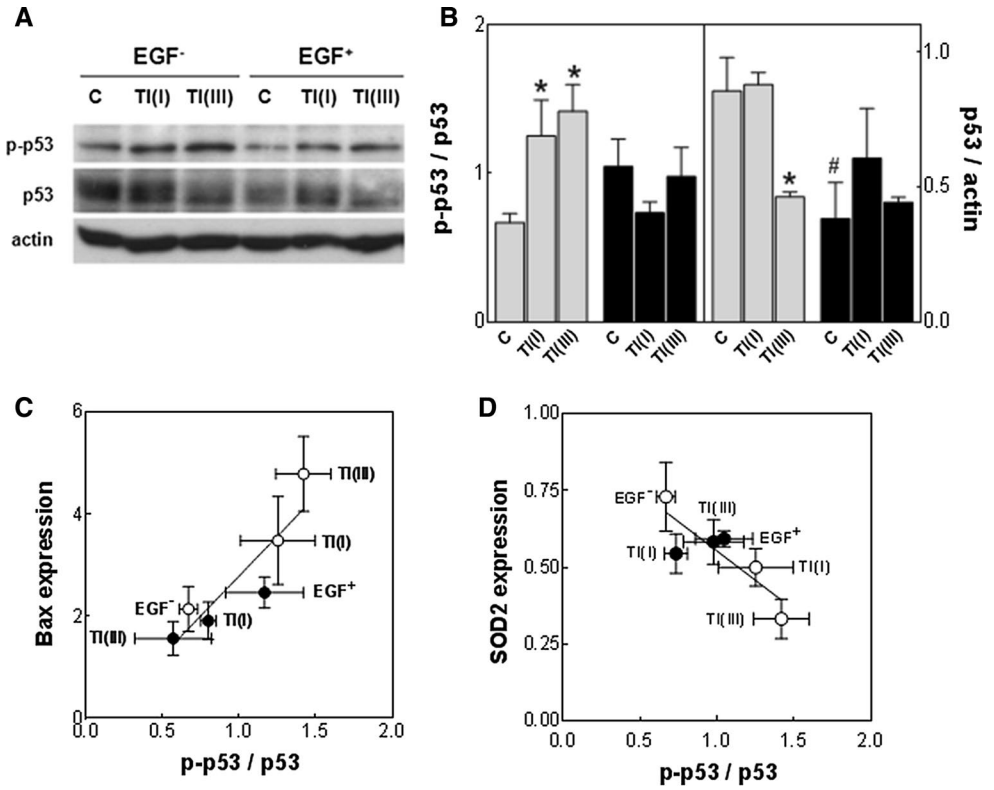

Fig. 7 EGF prevents Tl-induced increase in p53 phosphorylation. PC12 cells were incubated at 37 °C for 24 h in serum-free DMEM. After media replacement, EGF^- (*white bar*) and EGF^+ (*black bar*) cells were further incubated for 24 h in the presence of 100 μM Tl(I) or Tl(III), and p53 phosphorylation and expression levels were evaluated. **a** Representative Western blots showing the region of the membrane corresponding to p-p53 and p53 (53 kDa) and actin (42 kDa) migration. **b** Relative p53 phosphorylation and expression content in Tl(I)- or Tl(III)-treated cells. Correlations between p53 phosphorylation and **c** Bax and **d** SOD2 expression in EGF^- (*open circle*) and EGF^+ (*filled circle*) cells exposed to 100 μM Tl(I) or Tl(III) (data taken from Figs. 3 and 4). Results are shown as the mean ± SEM of at least four independent experiments. *Asterisk* denotes a significant difference from the value measured in control cells ($P < 0.05$). *Number sign* denotes a significant difference from the value measured in EGF^- cells ($P < 0.05$)

Tl(III) for all the concentrations assessed ($P < 0.01$; Fig. 6f, g). In EGF^+ cells, Tl(I) (10–25 μM) had a modest effect on p38 phosphorylation (+163 and +134 %, $P < 0.001$ respect to the controls). In contrast, 100 μM Tl(III) markedly promoted p38 phosphorylation (+360 %, $P < 0.001$ respect to the controls) in EGF^+ cells. No significant differences were found between the magnitude of Tl(III)-mediated p38 phosphorylation in EGF^- and EGF^+ cells.

The expression and activation levels of the protein p53 were also investigated. In EGF^+ cells, basal levels of p53 were 55 % lower than in EGF^- cells ($P < 0.05$; Fig. 7b). In EGF^- cells, only Tl(III) affected p53 expression (−46 %, $P < 0.05$ respect to controls), with no changes observed for the other conditions assessed (Fig. 7b). In EGF^- cells, both Tl(I) and Tl(III) markedly increased p53 phosphorylation (+87 and +110 %, respectively; $P < 0.05$), an effect that was absent in EGF^+ cells. Significant correlations were observed between the extent of p53 phosphorylation and Bax (r^2: 0.81, $P < 0.05$; Fig. 7c) and SOD2 (r^2: 0.72, $P < 0.05$; Fig. 7d) expression levels. As an increase in p53 phosphorylation can induce senescence, we evaluated the amount of senescent cells in the samples from the activity of SA-β-Gal. In EGF^- cells, approximately 1.2 % of cells were senescent (Fig. 8) and this amount increased up to 4.5 % ($P < 0.001$) when exposed to 100 μM Tl(III). This effect of Tl(III) was prevented when cells were either pre-incubated with an inhibitor of p53 (pifithrin-α) or added with EGF (Fig. 8). Tl(I) induced cell senescence in neither EGF^- nor EGF^+ cells (Fig. 8).

Finally, the participation of ERK1/2, JNK, p38, and p53 on Tl-mediated apoptosis in EGF^- and EGF^+ cells was further characterized using specific inhibitors. In both EGF^- (Fig. 9a) and EGF^+ (Fig. 9b) cells, the inhibition of p53 (pifithrin-α), ERK1/2 (PD98059), JNK (SP600125), or p38 (SB203580) prevented 100 μM Tl(I)-induced apoptosis, suggesting that the activation of all these pathways acts jointly to cause apoptosis. In contrast, the pro-apoptotic effect of 100 μM Tl(III) was not affected by the inhibition of p53, ERK1/2, or JNK (Fig. 9a, b). However, it was prevented when EGF^- or EGF^+ cells were treated with p38

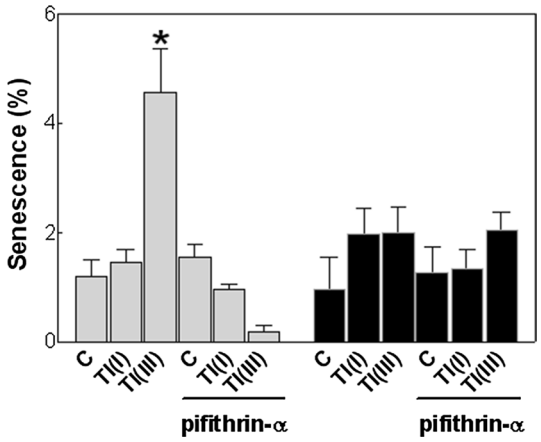

Fig. 8 EGF prevents Tl(III)-induced cell senescence. PC12 cells were incubated at 37 °C for 24 h in serum-free DMEM. After media replacement, EGF^- (*white bar*) and EGF^+ (*black bar*) cells were further incubated for 24 h in the presence of 100 μM Tl(I) or Tl(III) in either the absence or presence of p53 inhibitor pifithrin-α (50 μM). Cells positive for SA-β-Gal activity determination were considered senescent. Results are shown as the mean ± SEM of at least four independent experiments. *Asterisk* denotes a significant difference from the value measured in control cells ($P < 0.05$)

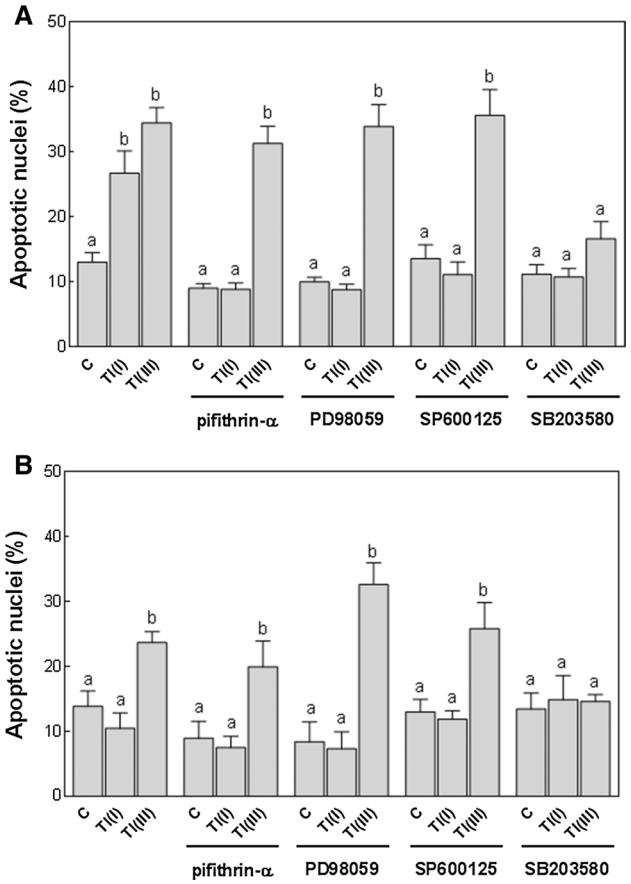

Fig. 9 Participation of p53, ERK1/2, JNK, and p38 in Tl(I)- and Tl(III)-mediated apoptosis. PC12 cells were incubated at 37 °C for 24 h in serum-free DMEM. After media replacement, **a** EGF^- and **b** EGF^+ cells were further incubated for 30 h in the presence of the following inhibitors: pifithrin-α (50 μM), PD98059 (10 μM), SP600125 (2 μM), or SB20358 (5 μM), either with or without the addition of 100 μM Tl(I) or Tl(III). The content of hypodiploid cells in the samples was evaluated by flow cytometry. Results are shown as the mean ± SEM of four independent experiments. *a* is significantly different from *b* ($P < 0.01$)

inhibitor, suggesting that the activation of this pathway is key in Tl(III)-induced apoptosis.

Discussion

Tl causes apoptosis in diverse cell types, including human leukemia T (Jurkat) cells (Bragadin et al. 2003), C6 glioma cells (Chia et al. 2005), cultured rat hepatocytes (Pourahmad et al. 2010; Eskandari et al. 2011), and PC12 cells (Hanzel and Verstraeten 2009; Hanzel et al. 2012). Similar to other toxic heavy metals, Tl(I) and Tl(III) induce mitochondrial destabilization with the subsequent enhancement of cell oxidant production (Hanzel and Verstraeten 2006; Pourahmad et al. 2010; Eskandari et al. 2011) which ultimately leads to the activation of the intrinsic (mitochondrial) pathway of apoptosis. In addition, Tl(III) triggers the extrinsic pathway and promotes lysosomal destabilization that participates in the activation of pro-apoptotic signals (Hanzel and Verstraeten 2009; Hanzel et al. 2012).

The mitogenic effect of EGF and the signaling pathways activated by this growth factor are well characterized in diverse cellular models, including PC12 cells (for a review, see Henson and Gibson 2006). We hypothesized that, in addition to be a mitogen, EGF may exert some protective effects against cytotoxic compounds. Worth of noticing, the doubling time of PC12 cells was calculated in 36–40 h (Mouri and Sako 2013; Pino and Verstraeten 2015). Therefore, at the time point selected for the studies in this work (24 h post-cell-cycle resumption), cell cycle was completed for neither EGF^- nor EGF^+ cells, with comparable amounts of cells expected in both experimental situations. MTT metabolization and Neutral red uptake measurements confirmed that similar amounts of viable cells were present in EGF^- and EGF^+ cells.

The loss of cell viability found after 24 h of cell exposure to Tl(I) can be considered marginal. For example, cell capacity to metabolize MTT upon the exposure to Tl(I) (100 μM) was decreased by 10 and 5 % in EGF^- and EGF^+ cells, respectively, while the uptake of Neutral red was reduced by 20 and 9 % in EGF^- and EGF^+ cells, respectively. This effect of Tl(I) was markedly lower than in our previous findings in non-synchronized PC12 cells where the decrease in mitochondrial functionality caused by 100 μM Tl(I) was ~25 % (Hanzel and Verstraeten 2006), suggesting a differential susceptibility

of synchronous and non-synchronous cell cultures to the toxic effects of Tl(I). In contrast, the extent of the loss of mitochondrial function in EGF^- cells exposed to 100 μM Tl(III) was considerably higher than that measured in non-synchronized cells (−44 % in EGF^- cells vs. −13 % in non-synchronized cells) (Hanzel and Verstraeten 2006). At this concentration, the loss of mitochondrial functionality in EGF^- cells was accompanied by decreased lysosomal functionality (−40 %) and compromised plasma membrane integrity (+24 %). These findings suggest that the entry of Tl(III) may occur at different time points of the cycle and/or by different routes than those of Tl(I) (Repetto et al. 1998). One of the routes participating in Tl(III) uptake in PC12 cells involves its interaction with the iron transport protein, transferrin (Hanzel et al. 2012). During the phase G_0 of the cycle, cells usually express low levels of transferrin receptors (TfR1 and TfR2). At the end of G_1, the expression of the high-affinity TfR1 starts (Neckers and Cossman 1983), followed by the expression of the low-affinity TfR2 during the S phase (Kawabata et al. 2000). Therefore, the increased expression of both receptors after cell cycle reentry would enhance Tl(III) uptake. Despite the possibility of Tl(III) being taken up in higher amounts during late G_1 and S phases, the loss of mitochondrial and lysosomal functionality along with the preservation of plasma membrane integrity due to Tl(III) in EGF^+ cells was lower than that in EGF^- cells. Hence, these findings support the hypothesis that this growth factor may prevent, or at least attenuate, the activation of signaling pathways triggered by Tl(III) that conduct cells to death.

Tl(III), and to a lesser extent Tl(I), affected the integrity of intracellular acidic compartments (endosomes and lysosomes) in EGF^- cells, an effect that was prevented by EGF. The destabilization of those compartments can be caused by several endogenous and exogenous factors, including increased steady-state levels of intracellular oxidants (Guicciardi et al. 2004). Consequently, acidic proteases including the cathepsins are released to the cytosol triggering a signaling cascade that activates the mitochondrial-dependent pathway of apoptosis (Repnik et al. 2012). The magnitude of lysosomal damage will determine cell fate. While discrete alterations of lysosomes cause apoptosis, massive destruction of those compartments causes necrosis (Guicciardi et al. 2004). Ultimately, affected cells will lose their capacity to maintain plasma membrane integrity and selectivity, and large non-permeable molecules (e.g., PI) will permeate through them and eventually exacerbate cell damage. The loss of mitochondrial and lysosomal functionality in cells exposed to Tl, together with the alteration of plasma membrane integrity, is indicators of a loss of cell viability, but they do not discriminate between apoptosis and necrosis.

The impact of Tl(I) and Tl(III) on mitochondrial functionality was investigated more extensively from the alterations in mitochondrial transmembrane potential, the production of oxidants, and the balance between the pro- and anti-apoptotic members of Bcl-2 family. Upon interaction with mitochondrial membrane, pro-apoptotic Bcl-2 proteins facilitate the release of cytochrome c to cytoplasm, which triggers the intrinsic pathway (Martinou and Youle 2011; Zhou et al. 2011). Similar to the observed previously, both Tl(I) and Tl(III) decreased mitochondrial potential in EGF^- cells but with a magnitude that was lower than that measured in non-synchronized cells (Hanzel and Verstraeten 2006). Mitochondrial oxidant production was also enhanced in these cells, the magnitude of the effect being higher than that measured in non-synchronized cells (Tl(I): +22 vs. +41 % in non-synchronized and EGF^- cells, respectively; Tl(III): +43 vs. +58 % in non-synchronized and EGF^- cells, respectively) (Hanzel and Verstraeten 2006). At the highest concentration assessed, the magnitude of the effect of the cations on mitochondrial depolarization and oxidant production was comparable to that caused by mitochondrial uncoupler DNP in these cells. Even when EGF prevented those noxious effects of Tl, it was unable to prevent mitochondrial depolarization and oxidant production by DNP. This finding suggests that, unlike DNP, Tl(I) and Tl(III) do not interact directly with mitochondria to cause their depolarization. Instead, Tl may have an indirect effect by activating certain signals that ultimately affect mitochondrial potential. The activation of these signals seems to be prevented by EGF, as evidenced from the normal mitochondrial potential found in EGF^+ cells exposed to Tl.

Because of mitochondrial depolarization, reactive oxygen species (ROS) are generated, including superoxide anion ($O_2^{\cdot-}$) and H_2O_2. The probe DHR123 is widely used for H_2O_2 detection but it also reacts with another highly oxidant species, the peroxynitrite anion ($ONOO^{\cdot-}$) (Glebska and Koppenol 2003). Hence, increased production of $ONOO^{\cdot-}$ could account for the observed effect in the current model. This possibility is in agreement with the decreased expression of SOD2 in EGF^- cells exposed to Tl(III), as this enzyme is responsible for $O_2^{\cdot-}$ metabolization into H_2O_2. In case of SOD2 expression—and hence, its activity—being decreased, H_2O_2 will be generated in lower amounts. Thus, the excess of $O_2^{\cdot-}$ will react rapidly with nitric oxide (NO; k: 6.7×10^9 M^{-1} s^{-1}) (Huie and Padmaja 1993) in a non-enzymatic reaction, generating $ONOO^{\cdot-}$ that will be detected by DHR123. Supporting that the amount of nitrite—final product of NO metabolism—released to the culture media was significantly increased in EGF^- cells exposed to Tl(III), an effect that was prevented by the inhibition of nitric oxide synthase (NOS) activity with L-NAME. On the other hand, Tl(I)-exposed cells had

slightly decreased expression of SOD2 and unaltered NOS activity. Therefore, the oxidation of DHR123 in EGF^- cells could be mostly ascribed to H_2O_2 in Tl(I)-treated cells and to $ONOO^{\cdot-}$ in Tl(III)-treated cells. The role of NO in the early steps of Tl-mediated cytotoxicity is currently under investigation.

Proteins belonging to the Bcl-2 family are involved in the regulation of mitochondrial-dependent apoptosis. The regulatory mechanisms exerted by these proteins are complex and include—but are not limited to—misbalances between the relative expression of the anti-apoptotic (e.g., Bcl-2 and Bcl-XL) and pro-apoptotic (e.g., Bax) members (reviewed in Chi et al. 2014; and Moldoveanu et al. 2014). In an attempt to overcome the toxicity of Tl(III), non-synchronized PC12 cells rapidly increase the relative amount of Bcl-2 respect to Bax, an effect that reaches a maximum at 6 h of cell exposure to Tl and that returns to control values at 24 h (Hanzel and Verstraeten 2009). EGF^- cells exposed to Tl(I) for 24 h had increased expression levels of Bcl-2 although with preserved degree of phosphorylation. In these cells, the increased levels of Bcl-2 were partially compensated by decreased expression levels of Bcl-XL, thus preserving the ratio between the pro- and anti-apoptotic Bcl-2 proteins. If Tl(I) affected the balance between pro- and anti-apoptotic Bcl-2 proteins in EGF^- cells, this effect occurred at earlier times of exposure, as observed in non-synchronized PC12 cells (Hanzel and Verstraeten 2009). On the other hand, at this time point, Tl(III) did not affect Bcl-2 and Bcl-XL expression but increased Bax expression, thus leading to a pro-apoptotic state. As Bcl-2 binds to Bax and prevents its oligomerization in mitochondrial outer membrane (Chi et al. 2014), the excess of Bax found in Tl(III)-treated EGF^- cells will be free to oligomerize into mitochondria membrane. The so-generated pores allow the release of cytochrome c and other apoptotic proteins to the cytosol with the consequent triggering of caspase-dependent and independent processes (Hanzel and Verstraeten 2009; Martinou and Youle 2011).

As mentioned in the Introduction, EGF rapidly activates the cascade Ras → Raf → MEK1/2 → ERK1/2, reaching a maximum around 10 min post-EGF treatment and becoming inactive at the G_1/S transition (Mebratu and Tesfaigzi 2009). This initial and limited activation of ERK1/2 is associated with cell survival and proliferation, while sustained activation of these kinases are implicated in cell apoptosis. In fact, a positive association has been established between the sustained phosphorylation of ERK1/2 and the activation of the pro-apoptotic p53 and Bax, as well as the activation of caspase 8 (Krishna and Narang 2008 and references therein). In addition to promote a rapid phosphorylation of ERK1/2 in EGF^- cells (Pino and Verstraeten 2015), Tl(I) also caused in these cells a long-term activation of ERK1/2. A relationship between enhanced oxidant production and ERK1/2 phosphorylation has been evidenced in diverse experimental models. For example, Fang et al. (2004) showed that the phosphorylation of ERK1/2 in rat hepatocytes exposed to the bile salts sodium deoxycholate or taurodeoxycholate was prevented by ROS scavengers. Likewise, the exposure of PC12 cells to the pro-oxidants $ONOO^{\cdot-}$ (Cerioni et al. 2003) or $CoCl_2$ (Lan et al. 2011) enhanced ERK1/2 phosphorylation in a ROS-dependent process. In contrast, the overexpression of SOD2 in mouse fibroblast (L929) cells prevented ROS-mediated ERK1/2 phosphorylation (Lee et al. 2004). Altogether, experimental results suggest that the increased H_2O_2 production observed in EGF^- cells exposed to Tl(I) may be responsible for the modest but sustained ERK1/2 activation which could contribute to the promotion of apoptosis in these cells.

In addition to ERK1/2, JNK and p38 were also activated in EGF^- cells exposed to Tl(I). The activation of JNK and p38 occurs in response to genotoxic and environmental stresses, including oxidative stress, UV radiation, heat shock, proinflammatory cytokines, and is mediated by a common MAPKKK, the apoptotic signal-regulating kinase 1 (ASK-1) (Matsuzawa and Ichijo 2008; Wagner and Nebreda 2009). The magnitude and duration of JNK and p38 activation will determine the fate of cells, as they control cell proliferation, differentiation, migration, and apoptosis (Lan et al. 2011). As expected in non-stressed cells, basal activation levels of JNK and p38 were similar in EGF^- and EGF^+ cells. The effects of the cations on JNK and p38 phosphorylation were different depending on the cation assessed and on the presence of EGF in the media. Tl(I) promoted JNK phosphorylation only in EGF^-. To notice, whereas the activation of p38 in Tl(I)-treated cells was prevented by EGF, the activation of p38 in Tl(III)-treated cells was unresponsive to EGF. The differential effect of the cations on p38 activation suggests that this particular MAPK may be activated by different signaling pathways in Tl(I)- and Tl(III)-exposed cells.

The number of cellular processes regulated by the tumor-suppressor protein p53 are continuously growing, not only as a key regulator of apoptosis but also as a promoter of cell survival and senescence (for a recent review, see Kruiswijk et al. 2015). Even though basal levels of nuclear p53 were higher in EGF^+ cells than in EGF^- cells, Tl(I) and Tl(III) affected p53 expression levels only in EGF^- cells. This protein has a short half-life (6–20 min), but it can be stabilized and activated upon phosphorylation on Ser_{15} by p-ERK1/2 (Cagnol and Chambard 2010). As a transcription factor, p53 regulates mitochondrial-dependent apoptosis at multiple levels (Galluzzi et al. 2011), and the outcome of the cells will be determined by the strength of the apoptotic stimuli. For example, under mild stress conditions p53 exerts cytoprotective actions by

stimulating the expression of damage-repairing enzymes, thus supporting cell survival. Upon severe acute oxidative stress, p53 transactivates genes encoding for certain pro-oxidant enzymes, upregulates the expression of the pro-apoptotic members of the Bcl-2 family, and represses the transcription of several redox-related genes (Galluzzi et al. 2011 and references therein), thus promoting apoptosis. Among others, p53 interacts with the promoter of Bax and enhances its transcription (Beckerman and Prives 2010). In the current model, a significant and positive correlation was observed between p53 phosphorylation and Bax expression, suggesting that this transcription factor may be involved in Tl-mediated mitochondrial apoptosis. In addition, phosphorylated p53 can prevent the transcription of *SOD2* gene (Drane et al. 2001). In line with this, increased SOD2 activity was observed in the liver of p53-deficient mice, whereas decreased SOD2 expression and activity were found upon a transient transfection of p53 gene in HeLa cells (Pani et al. 2000). In addition to regulate SOD2 at the transcription level, p53 binds to SOD2 in mitochondria and inhibits its activity (Zhao et al. 2005). A regulatory role of p53 on SOD2 expression seems to be operative in the current experimental model, as inferred from the negative correlation observed between p53 phosphorylation and SOD2 expression levels. As mentioned above, p53 is also a key mediator of cell senescence via the induction of p21, a cell cycle inhibitor that causes the arrest of the cycle at the G1/S phase transition (Aravinthan 2015). In EGF^- cells, Tl(III)—but not Tl(I)—increased the amount of senescent cells, an effect that was prevented by p53-specific inhibitor pifithrin-α. In line with the normal levels of p53 found in EGF^+ cells, no alterations in the number of senescent cells were observed upon the exposure to Tl. Although the increase in the amount of senescent cells in this particular cell line is small, senescence induction is another mechanism that appears to contribute to Tl(III) toxicity, by withdrawing cells from the normal progression of cell cycle.

Finally, the individual participation of the MAPKs and p53 in Tl(I)- and Tl(III)-mediated apoptosis was investigated in the current model using specific inhibitors of ERK1/2, JNK, p38, and p53. Interestingly, Tl(I)-mediated apoptosis was prevented by all the inhibitors assessed, which may imply that the activation of all these pathways is required to cause cell death upon Tl(I) exposure. In accordance with the negligible activation of ERK1/2 and JNK found in Tl(III)-exposed EGF^- cells, the inhibition of these MAPKs did not prevent apoptosis. In addition, although p53 phosphorylation was increased upon Tl(III) exposure, this transcription factor was not the main responsible for the promotion of apoptosis in this model, as evidenced from the lack of inhibition of apoptosis by pifithrin-α. Only when p38-dependent signaling was prevented by the specific inhibitor SB203580 the amount of apoptotic cells in Tl(III)-treated cells remained within control values. Among others, increased levels of $ONOO^{\cdot-}$ (Ghatan et al. 2000; Shacka et al. 2006) and increased Fas expression (Brenner et al. 1997) can activate p38. In turn, phosphorylated p38 redirects Bax to mitochondrial membrane where it triggers the intrinsic pathway of apoptosis in diverse cell models, including PC12 cells (Shacka et al. 2006). Since the enhanced production of $ONOO^{\cdot-}$ was indirectly corroborated from the increase in nitrite released to the culture media in both EGF^- and EGF^+ cells submitted to Tl(III), this oxidant may be at least partially account for p38-dependent cell apoptosis in Tl(III)-treated cells. In addition, by inhibiting p38 kinase activity with SB203580, Fas-triggered apoptosis can be aborted (Brenner et al. 1997), thus explaining the inhibition of apoptosis in Tl(III)-exposed cells upon p38 inhibition.

Altogether, experimental evidence presented in this work indicates that Tl(I) and Tl(III) promote apoptosis in EGF^- cells by activating different signaling pathways. Tl(I) caused a sustained activation of MAPKs and p53, promoted mitochondrial depolarization with the subsequent production of H_2O_2 and triggering of the intrinsic pathway. On the other hand, Tl(III) activated the extrinsic pathway, by increasing Fas content and activating caspase 8. In addition, Tl(III) promoted a sustained activation of p53 and p38, which may be mediated by increased content of nitrogen reactive species, such as $ONOO^{\cdot-}$ and/or by increased Fas levels. As p38 has been associated with Bax translocation to mitochondria and the activation of the mitochondrial apoptosis, the elucidation of this pathway helps to explain the mechanisms underlying Tl(III) toxicity. The presence of growth factors, such as EGF, has a modulatory role in the overall process by limiting—in magnitude and/or duration—the activation of pro-apoptotic signaling pathways caused by Tl and allowing cell survival.

Acknowledgments This work was supported by grants of Universidad de Buenos Aires (B086 and 20020100100112) and Agencia Nacional de Promoción Científica y Tecnológica (ANPCyT) (PICT 32273 and 2013–1018), Argentina. SVV is a career investigator of CONICET. Authors are grateful to Dr. Juan Pablo Carnevale, Dr. Ana M Adamo, Dr. Leonor Roguin and Dr. Johanna Miquet for the generous gift of etoposide, the antibodies against β-tubulin, ERK1/2, and p-p53, respectively.

Compliance with ethical standards

Conflict of interest The authors declare that they have no conflict of interest.

References

Aravinthan A (2015) Cellular senescence: a hitchhiker's guide. Hum Cell 28:51–64

ATSDR (1999) Thallium. ATSDR (Agency for Toxic Substances and Disease Registry). Prepared by Clement International Corp., under contract 205-88-0608, Atlanta, GA

Beckerman R, Prives C (2010) Transcriptional regulation by p53. Cold Spring Harb Perspect Biol 2:a000935

Bradford MM (1976) A rapid and sensitive method for the quantitation of microgram quantities of protein utilizing the principle of protein-dye binding. Anal Biochem 72:248–254

Bragadin M, Toninello A, Bindoli A, Rigobello MP, Canton M (2003) Thallium induces apoptosis in Jurkat cells. Ann N Y Acad Sci 1010:283–291

Brenner B, Koppenhoefer U, Weinstock C, Linderkamp O, Lang F, Gulbins E (1997) Fas- or ceramide-induced apoptosis is mediated by a Rac1-regulated activation of Jun N-terminal kinase/p38 kinases and GADD153. J Biol Chem 272:22173–22181

Bunzl K, Trautmannsheimer M, Schramel P, Reifenhäuser W (2001) Availability of arsenic, copper, lead, thallium, and zinc to various vegetables grown in slag-contaminated soils. J Environ Qual 30:934–939

Cagnol S, Chambard JC (2010) ERK and cell death: mechanisms of ERK-induced cell death-apoptosis, autophagy and senescence. FEBS J 277:2–21

Cerioni L, Palomba L, Cantoni O (2003) The Raf/MEK inhibitor PD98059 enhances ERK1/2 phosphorylation mediated by peroxynitrite via enforced mitochondrial formation of reactive oxygen species. FEBS Lett 547:92–96

Cheam V (2001) Thallium contamination of water in Canada. Water Qual Res J Can 36:851–877

Chen TK, Luo G, Ewing AG (1994) Amperometric monitoring of stimulated catecholamine release from rat pheochromocytoma (PC12) cells at the zeptomole level. Anal Chem 66:3031–3035

Chi X, Kale J, Leber B, Andrews DW (2014) Regulating cell death at, on, and in membranes. Biochim Biophys Acta 1843:2100–2113

Chia CF, Chen SC, Chen CS, Shih CM, Lee HM, Wu CH (2005) Thallium acetate induces C6 glioma cell apoptosis. Ann N Y Acad Sci 1042:523–530

Ciapetti G, Granchi D, Verri E, Savarino L, Cavedagna D, Pizzoferrato A (1996) Application of a combination of neutral red and amido black staining for rapid, reliable cytotoxicity testing of biomaterials. Biomaterials 17:1259–1264

Cvjetko P, Cvjetko I, Pavlica M (2010) Thallium toxicity in humans. Arh Hig Rada Toksikol 61:111–119

Dimri GP, Lee X, Basile G et al (1995) A biomarker that identifies senescent human cells in culture and in aging skin in vivo. Proc Natl Acad Sci USA 92:9363–9367

Drane P, Bravard A, Bouvard V, May E (2001) Reciprocal down-regulation of p53 and SOD2 gene expression-implication in p53 mediated apoptosis. Oncogene 20:430–439

Eskandari MR, Pourahmad J, Daraei B (2011) Thallium(I) and thallium(III) induce apoptosis in isolated rat hepatocytes by alterations in mitochondrial function and generation of ROS. Toxicol Environ Chem 93:145–156

Fang Y, Han SI, Mitchell C et al (2004) Bile acids induce mitochondrial ROS, which promote activation of receptor tyrosine kinases and signaling pathways in rat hepatocytes. Hepatology 40:961–971

Fujita K, Lazarovici P, Guroff G (1989) Regulation of the differentiation of PC12 pheochromocytoma cells. Environ Health Perspect 80:127–142

Galluzzi L, Morselli E, Kepp O, Vitale I, Pinti M, Kroemer G (2011) Mitochondrial liaisons of p53. Antioxid Redox Signal 15:1691–1714

Galvan-Arzate S, Santamaria A (1998) Thallium toxicity. Toxicol Lett 99:1–13

Ghatan S, Larner S, Kinoshita Y et al (2000) p38 MAP kinase mediates bax translocation in nitric oxide-induced apoptosis in neurons. J Cell Biol 150:335–347

Glebska J, Koppenol WH (2003) Peroxynitrite-mediated oxidation of dichlorodihydrofluorescein and dihydrorhodamine. Free Radic Biol Med 35:676–682

Greene LA, Tischler AS (1976) Establishment of a noradrenergic clonal line of rat adrenal pheochromocytoma cells which respond to nerve growth factor. Proc Natl Acad Sci USA 73:2424–2428

Guevara I, Iwanejko J, Dembinska-Kiec A et al (1998) Determination of nitrite/nitrate in human biological material by the simple Griess reaction. Clin Chim Acta 274:177–188

Guicciardi ME, Leist M, Gores GJ (2004) Lysosomes in cell death. Oncogene 23:2881–2890

Hanzel CE, Verstraeten SV (2006) Thallium induces hydrogen peroxide generation by impairing mitochondrial function. Toxicol Appl Pharmacol 216:485–492

Hanzel CE, Verstraeten SV (2009) Tl(I) and Tl(III) activate both mitochondrial and extrinsic pathways of apoptosis in rat pheochromocytoma (PC12) cells. Toxicol Appl Pharmacol 236:59–70

Hanzel CE, Almeira Gubiani MF, Verstraeten SV (2012) Endosomes and lysosomes are involved in early steps of Tl(III)-mediated apoptosis in rat pheochromocytoma (PC12) cells. Arch Toxicol 86:1667–1680

Heim M, Wappelhorst O, Markert B (2002) Thallium in terrestrial environments—occurrence and effects. Ecotoxicology 11:369–377

Henson ES, Gibson SB (2006) Surviving cell death through epidermal growth factor (EGF) signal transduction pathways: implications for cancer therapy. Cell Signal 18:2089–2097

Huie RE, Padmaja S (1993) The reaction of NO with superoxide. Free Radic Res Commun 18:195–199

Kawabata H, Germain RS, Vuong PT, Nakamaki T, Said JW, Koeffler HP (2000) Transferrin receptor 2-alpha supports cell growth both in iron-chelated cultured cells and in vivo. J Biol Chem 275:16618–16625

Krishna M, Narang H (2008) The complexity of mitogen-activated protein kinases (MAPKs) made simple. Cell Mol Life Sci 65:3525–3544

Kruiswijk F, Labuschagne CF, Vousden KH (2015) p53 in survival, death and metabolic health: a lifeguard with a licence to kill. Nat Rev Mol Cell Biol 16:393–405

Lan A, Liao X, Mo L et al (2011) Hydrogen sulfide protects against chemical hypoxia-induced injury by inhibiting ROS-activated ERK1/2 and p38MAPK signaling pathways in PC12 cells. PLoS One 6:e25921

Law S, Turner A (2011) Thallium in the hydrosphere of south west England. Environ Pollut 159:3484–3489

Lee YJ, Cho HN, Jeoung DI et al (2004) HSP25 overexpression attenuates oxidative stress-induced apoptosis: roles of ERK1/2 signaling and manganese superoxide dismutase. Free Radic Biol Med 36:429–444

Martinou JC, Youle RJ (2011) Mitochondria in apoptosis: Bcl-2 family members and mitochondrial dynamics. Dev Cell 21:92–101

Matsuzawa A, Ichijo H (2008) Redox control of cell fate by MAP kinase: physiological roles of ASK1-MAP kinase pathway in stress signaling. Biochim Biophys Acta 1780:1325–1336

Mebratu Y, Tesfaigzi Y (2009) How ERK1/2 activation controls cell proliferation and cell death: is subcellular localization the answer? Cell Cycle 8:1168–1175

Moldoveanu T, Follis AV, Kriwacki RW, Green DR (2014) Many players in BCL-2 family affairs. Trends Biochem Sci 39:101–111

Mosmann T (1983) Rapid colorimetric assay for cellular growth and survival: application to proliferation and cytotoxicity assays. J Immunol Methods 65:55–63

Mouri K, Sako Y (2013) Optimality conditions for cell-fate heterogeneity that maximize the effects of growth factors in PC12 cells. PLoS Comput Biol 9:e1003320

Neckers LM, Cossman J (1983) Transferrin receptor induction in mitogen-stimulated human T lymphocytes is required for DNA

synthesis and cell division and is regulated by interleukin 2. Proc Natl Acad Sci U S A 80:3494–3498

Nicoletti I, Migliorati G, Pagliacci MC, Grignani F, Riccardi C (1991) A rapid and simple method for measuring thymocyte apoptosis by propidium iodide staining and flow cytometry. J Immunol Methods 139:271–279

Pani G, Bedogni B, Anzevino R et al (2000) Deregulated manganese superoxide dismutase expression and resistance to oxidative injury in p53-deficient cells. Cancer Res 60:4654–4660

Pavlickova J, Zbiral J, Smatanova M, Habarta P, Houserova P, Kuban V (2006) Uptake of thallium from naturally-contaminated soils into vegetables. Food Addit Contam 23:484–491

Peter AL, Viraraghavan T (2005) Thallium: a review of public health and environmental concerns. Environ Int 31:493–501

Pino MT, Verstraeten SV (2015) Tl(I) and Tl(III) alter the expression of EGF-dependent signals and cyclins required for pheochromocytoma (PC12) cell-cycle resumption and progression. J Appl Toxicol 35:952–969

Pourahmad J, Eskandari MR, Daraei B (2010) A comparison of hepatocyte cytotoxic mechanisms for thallium (I) and thallium (III). Environ Toxicol 25:456–467

Queirolo F, Stegen S, Contreras-Ortega C, Ostapczuk P, Queirolo A, Paredes B (2009) Thallium levels and bioaccumulation in environmental samples of northern Chile: human health risks. J Chil Chem Soc 54:464–469

Rago RP, Brazy PC, Wilding G (1992) Disruption of mitochondrial function by suramin measured by rhodamine 123 retention and oxygen consumption in intact DU145 prostate carcinoma cells. Cancer Res 52:6953–6955

Repetto G, Del Peso A, Repetto M (1998) Human thallium toxicity. In: Nriagu J (ed) Thallium in the environment advances in environmental science and technology. Wiley, New York, pp 167–199

Repetto G, del Peso A, Zurita JL (2008) Neutral red uptake assay for the estimation of cell viability/cytotoxicity. Nat Protoc 3:1125–1131

Repnik U, Stoka V, Turk V, Turk B (2012) Lysosomes and lysosomal cathepsins in cell death. Biochim Biophys Acta 1824:22–33

Sabbioni E, Marafante E, Rade J, Di Nucci A, Gregotti C, Manzo L (1981) Metabolic patterns of low and toxic doses of thallium in the rat. In: Holmstedt B, Lauwerys R, Mercier M, Roberfroid M (eds) Mechanisms of Toxicity and Hazard Evaluation. Elsevier, North-Holland, pp 559–564

Schaub G (1996) Effects on humans. In: Schaub G (ed) Thallium Environmental Health Criteria, vol 182. World Health Organization, Geneva, pp 147–168

Shacka JJ, Sahawneh MA, Gonzalez JD, Ye YZ, D'Alessandro TL, Estevez AG (2006) Two distinct signaling pathways regulate peroxynitrite-induced apoptosis in PC12 cells. Cell Death Differ 13:1506–1514

Verstraeten SV (2006) Relationship between thallium(I)-mediated plasma membrane fluidification and cell oxidants production in Jurkat T cells. Toxicology 222:95–102

Wagner EF, Nebreda AR (2009) Signal integration by JNK and p38 MAPK pathways in cancer development. Nat Rev Cancer 9:537–549

Wierzbicka M, Szarek-Lukaszewska G, Grodzinska K (2004) Highly toxic thallium in plants from the vicinity of Olkusz (Poland). Ecotoxicol Environ Saf 59:84–88

Xiao T, Guha J, Boyle D, Liu CQ, Chen J (2004) Environmental concerns related to high thallium levels in soils and thallium uptake by plants in southwest Guizhou, China. Sci Total Environ 318:223–244

Zhao Y, Chaiswing L, Velez JM et al (2005) p53 translocation to mitochondria precedes its nuclear translocation and targets mitochondrial oxidative defense protein-manganese superoxide dismutase. Cancer Res 65:3745–3750

Zhou F, Yang Y, Xing D (2011) Bcl-2 and Bcl-xL play important roles in the crosstalk between autophagy and apoptosis. FEBS J 278:403–413